Journal of Catalysis **187,** 151–159 (1999)
Article ID jcat.1999.2593, available online at http://www.idealibrary.com on IDEAL®

Effect of Support on Partial Oxidation of Methane to Synthesis Gas over Supported Rhodium Catalysts

E. Ruckenstein[1] and H. Y. Wang

Department of Chemical Engineering, State University of New York at Buffalo, Amherst, New York 14260

Received March 1, 1999; revised May 24, 1999; accepted May 25, 1999

Two kinds of oxides, reducible and irreducible, were used as supports. It was found that the reducible-oxides-supported rhodium catalysts provide, in general, much lower activities and selectivities than those supported on irreducible oxides. The exposed metal surface areas of the reduced catalysts were determined, and the reaction behaviors of CH_4/O_2 (2/1) over the pure supports and the precalcined 1% Rh(O)/M_xO_y catalysts were investigated in a pulse microreactor. It is suggested that the partial coverage of rhodium sites by the reducible oxides and the combustion of methane that occurs over these oxide sites are responsible for the lower activities and selectivities observed over this kind of supported catalysts. Among the irreducible metal oxides, γ-Al_2O_3, La_2O_3, and MgO provided stable catalytic activities and selectivities during 100 h of reaction, and the activity increased in the sequence $La_2O_3 < \gamma$-$Al_2O_3 \leq$ MgO. Possible explanations for stability are proposed on the basis of TPR and XRD experiments. In addition, the nature of the active sites is examined based on pulse reaction experiments. © 1999 Academic Press

Key Words: **methane partial oxidation; syngas; rhodium-based catalyst; effect of support.**

1. INTRODUCTION

Steam reforming constitutes the dominant commercial process employed to produce synthesis gas (a mixture of CO and H_2) from methane (1, 2):

$$CH_4 + H_2O \rightarrow CO + 3H_2 \quad \Delta H^0_{298} = 206 \text{ kJ/mol.} \quad [1]$$

However, this process requires a large energy input and provides a syngas with a too high H_2/CO ratio (>3) for the methanol and Fischer–Tropsch syntheses. For these reasons, research efforts have been made to obtain the suitable ratio of 2 via methane partial oxidation to H_2 and CO (3–28):

$$CH_4 + 1/2O_2 \rightarrow CO + 2H_2 \quad \Delta H^0_{298} = -36 \text{ kJ/mol.} \quad [2]$$

This reaction is mildly exothermic, and the catalysts were mainly supported noble metals, such as Rh, Ru, Pd, Pt (3–10), and supported Ni catalysts (11–23), as well as some pyrochlore-type oxides, such as $Ln_2Ru_2O_7$ (24, 25), and perovskite type oxides, such as $LaMO_3$ (M = Ni, Rh, Co, Cr) (26–28).

The support is usually a surface that allows the spreading of the metal catalyst as small clusters. In some cases, the support may actually contribute to the catalytic activity. For the CO_2 reforming of methane over Rh-based catalysts, the activity sequence of the supports was $Al_2O_3 > TiO_2 > SiO_2$ (29). For both the partial oxidation of methane and the CO_2 reforming of methane over Ir-based catalysts, the activity sequence was $TiO_2 \geq ZrO_2 \geq Y_2O_3 > La_2O_3 > MgO \geq Al_2O_3 > SiO_2$ (30). For the partial oxidation of hydrocarbons over noble metal monoliths, the effect of the support was small (31).

It is well known that, after a high-temperature H_2 reduction, the hydrogen and carbon monoxide chemisorption may be suppressed over the group VIII metal crystallites supported on semiconductor oxides (e.g., CeO_2, Nb_2O_5, Ta_2O_5, TiO_2, ZrO_2), without appreciable change in their dispersion (32, 33). Because this effect, called strong metal–support interactions (SMSI), can play an important role, it is of interest to compare the performances of group VIII metal catalysts supported on reducible and irreducible oxides in the partial oxidation of methane. In the present paper, two kinds of metal oxides, reducible and irreducible, were used as supports for rhodium. It was found that the irreducible oxides provided much higher activities and selectivities than the reducible ones. Among the irreducible oxides, γ-Al_2O_3 and MgO, exhibited high activities and selectivities with high stability. A somewhat lower activity but comparable selectivities and stability were provided by the La_2O_3 support. Possible explanations based on pulse reactions, CO chemisorption, TPR, and XRD experiments are suggested.

2. EXPERIMENTAL

2.1. Catalyst Preparation

The following supports were used: γ-Al_2O_3, CeO_2, Nb_2O_5, Ta_2O_5, ZrO_2 (Alfa); and La_2O_3, $MgO_2 \cdot x$MgO,

[1] To whom correspondence should be addressed.

0021-9517/99 $30.00
Copyright © 1999 by Academic Press
All rights of reproduction in any form reserved.

SiO_2, TiO_2, Y_2O_3 (Aldrich). The supported rhodium catalysts were prepared by impregnating the support with an ethanol solution of $Rh(NO_3)_3 \cdot 2H_2O$ (Alfa), followed by overnight drying at 110°C and calcination in air at 800°C for 4 h. The calcined catalysts are denoted $Rh(O)/M_xO_y$. Since $MgO_2 \cdot x$MgO was completely converted into MgO after calcination at 800°C for 4 h, its supported rhodium catalyst is also denoted Rh(O)/MgO. The catalysts reduced in H_2 are denoted Rh/M_xO_y. Rh loading means wt% Rh in the reduced catalyst.

2.2. Activity Assay

All activity assays were conducted under atmospheric pressure in a fixed-bed vertical quartz reactor (3 mm inside diameter) located in an electronically controlled furnace, with the catalyst powder held on quartz wool. Five (5.0) mg catalyst was used in each run. The prepared catalyst was heated in an H_2 flow (20 ml/min) up to 750°C at 20°C/min, after which, maintaining the furnace temperature at 750°C, H_2 was switched to a CH_4/O_2 mixture with a molar ratio of 2.0, at a GHSV of 720000 ml g^{-1} h^{-1}. The reactants and products were analyzed with an on-line gas chromatograph equipped with Porapak Q and 5A molecular sieve columns. A thermocouple was inserted into the middle of the catalyst bed to measure the temperature of the catalyst.

Methane (99.97% purity, from Matheson) and oxygen (99.9% purity, from Cryogenic) were used without further purification. The gases were premixed before they were introduced into the reactor.

2.3. Pulse Reaction

A quartz tube (4 mm inside diameter) was used as reactor with the calcined catalyst held on quartz wool. A constant flow of helium (35 ml/min) was employed, and a reactant gas mixture was injected in the carrier gas. In each run, 50.0 mg catalyst was used and the pulse volume was 50 μl CH_4/O_2 (2/1). The reactants and products were analyzed with an on-line gas chromatograph equipped with a thermal conductivity detector (TCD) and a Porapak Q column. The carrier gas helium was purified using Hydro-Purge II and Oxy-Trap columns.

2.4. Catalyst Characterization

2.4.1. Surface area. The surface areas of the calcined catalysts were determined by nitrogen adsorption, using a Micromeritics ASAP2000 instrument. The sample was degassed at 200°C for at least 5 h in high vacuum before the measurement.

2.4.2. The exposed metal surface area. The exposed surface areas of rhodium of the reduced catalysts were determined by CO chemisorption at room temperature by assumming a 1/1 stoichiometry. The exposed surface area of rhodium was calculated by assuming a hemisphere shape for the crystallites. One hundred (100.0) mg catalyst powder held on quartz wool was reduced in an H_2 flow (20 ml/min) at 550°C for 1.5 h. Further, at the same temperature, the reduced catalyst was purged with ultrahigh purity helium (35 ml/min) for 1 h. After the temperature was decreased to room temperature, CO (10 μl per pulse) was pulsed over the catalyst until no further adsorption of CO was detected. The CO left during CO chemisorption was determined quantitatively with a thermal conductivity detector (TCD). Both the hydrogen and helium were purified with Hydro-Purge II and Oxy-Trap columns before use.

2.4.3. Temperature-programmed reduction (TPR). The TPR of the catalyst was conducted by heating the calcined catalyst from 50 to 850°C at a rate of 20°C/min in a flow of 2.5% H_2/Ar mixture (35 ml/min). The hydrogen consumed in TPR was determined with a thermal conductivity detector (TCD). Fifty (50.0) mg sample precalcined in air at 800°C for 4 h was used in each TPR run.

2.4.4. X-ray powder diffraction (XRD). X-ray powder diffraction (XRD) was carried out on a Siemens D500 X-ray diffractometer, using Cu $K\alpha$ radiation, at 40 kV and 30 mA.

3. RESULTS

3.1. Continuous Reaction

3.1.1. Effect of support on the performance of Rh catalysts. Two kinds of metal oxides, reducible (e.g., CeO_2, Nb_2O_5, Ta_2O_5, TiO_2, and ZrO_2) and irreducible (e.g., γ-Al_2O_3, La_2O_3, MgO, SiO_2, Y_2O_3), were used as supports. As shown in Table 1, the performance of the supported rhodium catalyst is strongly affected by the support. Figure 1 shows the effect of time on stream on the activity of rhodium supported on the irreducible oxides and on the reducible Ta_2O_5. (The conversions in this paper have been always lower than the equilibrium conversions (34) at the temperatures of the catalysts.) The catalytic performances of the supported rhodium catalysts can be summarized as follows:

(i) With the exception of Ta_2O_5, the reducible oxides provided much lower methane conversions and selectivities to CO and H_2 than the irreducible ones (Table 1).

(ii) Nb_2O_5 and TiO_2 not only exhibited poor activities and selectivities to CO and H_2 but also provided a syngas with low H_2/CO ratio (1.0 and 1.5, respectively). The other supports provided an H_2/CO ratio of about 2, as expected from the stoichiometry of the reaction (Table 1).

(iii) Among the irreducible metal oxides, γ-Al_2O_3, La_2O_3, and MgO provided stable activities during 100 h of reaction, and the activity increased in the sequence $La_2O_3 < \gamma$-$Al_2O_3 \leq$ MgO; deactivation was observed over the SiO_2- and Y_2O_3-supported catalysts (Fig. 1).

TABLE 1

Activity of Supported Rh (1 wt%) Catalysts for Methane Partial Oxidation at 750°C ($T_{furnace}$)[a]

Catalysts	Surf. area (m^2/g-cat.)	Rh surf. area (m^2/g-cat. × 10^2)	Catal. temp. (°C)	CH_4 conv. (%)	CO select. (%)	H_2 select. (%)	H_2/CO (ratio)
Rh/CeO_2	3.2	2.7	796	58.1	71.6	72.1	2.0
Rh/Nb_2O_5	6.1	0.1	840	33.0	35.3	17.5	1.0
Rh/Ta_2O_5	5.0	—[b]	782	69.1	95.8	92.2	1.9
Rh/TiO_2	10.1	3.2	815	47.1	68.2	52.5	1.5
Rh/ZrO_2	4.1	2.4	770	55.4	72.7	69.4	1.9
Rh/Al_2O_3	59.3	28.1	759	81.6	94.0	93.5	2.0
Rh/La_2O_3	6.2	7.9	766	72.5	90.3	91.6	2.0
Rh/MgO	37.4	17.9	761	75.5	92.1	96.4	2.1
Rh/SiO_2	573.7	41.5	752	80.1	86.7	93.5	2.2
Rh/Y_2O_3	9.4	14.9	789	68.3	85.9	88.7	2.1

[a] Catalyst, 5.0 mg; flow rate, 60.0 ml/min ($CH_4/O_2 = 2.0$); space velocity, 720000 h^{-1} ml/g-catalyst; data obtained after 6 h of reaction; the oxygen conversion was always 100%.

[b] Data not obtainable because the reaction $2CO \rightarrow CO_2 + \underline{C}$ occurred over this catalyst at room temperature.

(iv) Though Ta_2O_5 provided much higher methane conversion and selectivities to CO and H_2 compared to the other reducible oxides, its activity decayed with time (Fig. 1).

(v) A relatively long induction time was observed over the MgO-supported rhodium catalyst.

3.2. Pulse Reaction

3.2.1. Reactivities of CH_4/O_2 (2/1) pulses over the oxide supports. The reaction of methane and oxygen over the metal oxides was investigated at 750 and 850°C by using pulses of CH_4/O_2 (2/1), and some results are listed in Table 2. The carbon balance indicated that no carbon deposition occurred during reaction. Except at 850°C over CeO_2, for which some CO and H_2 was formed, the products of the reaction during the first pulse were exclusively CO_2 and H_2O. Except with ZrO_2 at 750°C and with CeO_2 at

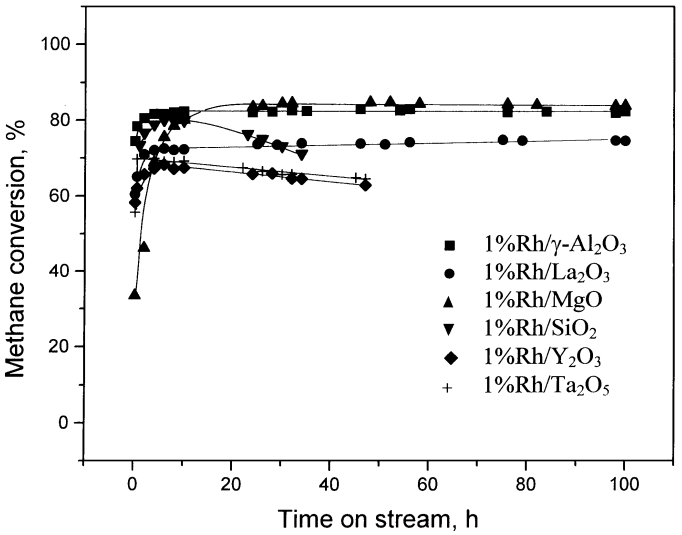

FIG. 1. Effect of time on stream on the activity of rhodium supported on the irreducible oxides and Ta_2O_5. $P = 1$ atm, $T_{furnace} = 750$°C, $CH_4/O_2 = 2.0$, GHSV = 720 000 ml g^{-1} h^{-1}.

TABLE 2

Reactivities of CH_4/O_2 (2/1) Pulses over Metal Oxides[a,b]

Supports	Surf. area[b] (m^2/g)	Temp. (°C)	CH_4 conv. (%)	O_2 conv. (%)	CO sel. (%)	CO_2 sel. (%)
CeO_2	3.3	750	21.9[c]	91.6	0.0	100.0
		850	51.2[c]	100.0	1.3	98.7
			44.6[d]	100.0	12.4	87.6
			32.7[e]	100.0	30.5	69.5
Nb_2O_5	4.9	750	6.1[c]	24.7	0.0	100.0
		850	13.6[c]	54.0	0.0	100.0
Ta_2O_5	3.8	750	—[f]	—	—	—
		850	1.0[c]	4.6	0.0	100.0
TiO_2	9.4	750	0.6[c]	2.6	0.0	100.0
		850	5.8[c]	24.3	0.0	100.0
ZrO_2	3.9	750	2.9[c]	2.8	0.0	100.0
		850	17.2[c]	62.0	0.0	100.0
γ-Al_2O_3	60.9	750	23.4[c]	88.8	0.0	100.0
		850	21.8[c]	82.1	0.0	100.0
La_2O_3	4.9	750	16.5[c]	76.1	0.0	100.0
		850	21.5[c]	86.9	0.0	100.0
MgO[g]	38.3	750	23.4[c]	93.5	0.0	100.0
		850	24.6[c]	92.3	0.0	100.0
SiO_2	594.0	750	9.0[c]	41.8	0.0	100.0
		850	16.0[c]	63.9	0.0	100.0
Y_2O_3	9.4	750	18.2[c]	88.5	0.0	100.0
		850	21.0[c]	81.4	0.0	100.0

[a] Catalysts, 50.0 mg; volume of CH_4/O_2 (2/1) pulse, 50.0 μl.

[b] After calcination at 800°C for 4 h.

[c] Data obtained for the first pulse.

[d] Data obtained for the second pulse.

[e] Data obtained for the third pulse.

[f] Almost no reaction occurred.

[g] Obtained from $MgO_2 \cdot x$MgO by calcination at 800°C for 4 h.

850°C, the conversion of O_2 was approximately four times that of CH_4, indicating that the overall reaction proceeded according to the combustion reaction,

$$CH_4 + 2O_2 = CO_2 + 2H_2O. \quad [3]$$

Among the reducible oxides, CeO_2 is the most reducible. At 850°C, CeO_2 was partially reduced by methane during the first pulse, as indicated by a methane conversion much higher than 25%. With the increase in the extent of reduction during successive pulses, the methane conversion decreased while the CO selectivity increased (Table 2).

Compared to the other reducible oxides, Ta_2O_5 exhibited much lower conversions of methane and oxygen; almost no reaction occurred at 750°C, and only 1.0% methane was converted at 850°C.

3.2.2. Reaction of CH_4/O_2 pulses over the 1 wt% $Rh(O)/M_xO_y$. The reaction between methane and oxygen over the oxidized catalysts was investigated by using CH_4/O_2 pulses with a stoichiometric feed ratio of 2/1. The products contained CO, H_2, CO_2, and H_2O. The carbon balance indicated that no carbon was deposited on the catalyst. In Figs. 2 and 3, the reactivities of CH_4/O_2 over the precalcined rhodium supported on irreducible and reducible oxides are compared at 750°C. Over the irreducible-oxide-supported catalysts, O_2 was completely converted during each pulse and the methane conversion was equal or close to 100% (Fig. 2a). During the first pulse, no CO or H_2 was formed, CO_2 being the only carbon-containing product (Fig. 2b). Starting with the second pulse, CO was formed and its selectivity increased rapidly over all the irreducible supports except MgO. Over the MgO-supported catalyst, no CO was formed until the fourth pulse. The high methane conversion (>95%) and CO selectivity (>92%) at the steady state over all the irreducible-oxide-supported rhodium catalysts indicate that the combustion reaction provides only a minor contribution. Among the reducible oxide supports, Ta_2O_5 exhibited reactivities similar to the irreducible ones (Fig. 3); this is consistent with the results of the continuous flow reaction (Table 1). Over the CeO_2- and ZrO_2-supported Rh catalysts, CO was formed starting with the third pulse and its selectivity greatly increased at the fourth pulse (Fig. 3c). Even though during the first two pulses the methane conversion was high (equal or close to 100%), it decreased notably starting with the third pulse. Both methane conversion and CO selectivity were much lower after the eighth pulse onward than those observed over the irreducible oxides (compare Figs. 3a and 3b to Fig. 2a); this is again consistent with the results of the continuous flow reaction (Table 1). Over the Nb_2O_5- and TiO_2-supported Rh catalysts, no H_2 or CO was formed, hence no partial oxidation reaction occurred (Fig. 3c). As over the pure reducible oxides (Table 2), the conversion of O_2 was approximately four times that of methane (Figs. 3a and 3b), indicating that the overall reaction proceeded according to the combustion reaction.

The effect of temperature on the reactivities of CH_4/O_2 (2/1) was also investigated. As shown in Fig. 4, over the γ-Al_2O_3-supported Rh catalyst, at both 650 and 750°C, CO was formed during the second pulse, but the CO selectivity was higher at 750°C than at 650°C. At 850°C, CO was formed during the first pulse. The higher the temperature, the more easily it induces the partial oxidation reaction. Similar results were observed over the other irreducible-oxide-supported rhodium catalysts.

As shown in Fig. 5, over the Nb_2O_5-supported rhodium catalyst, at 650 and 750°C, no H_2 or CO was formed,

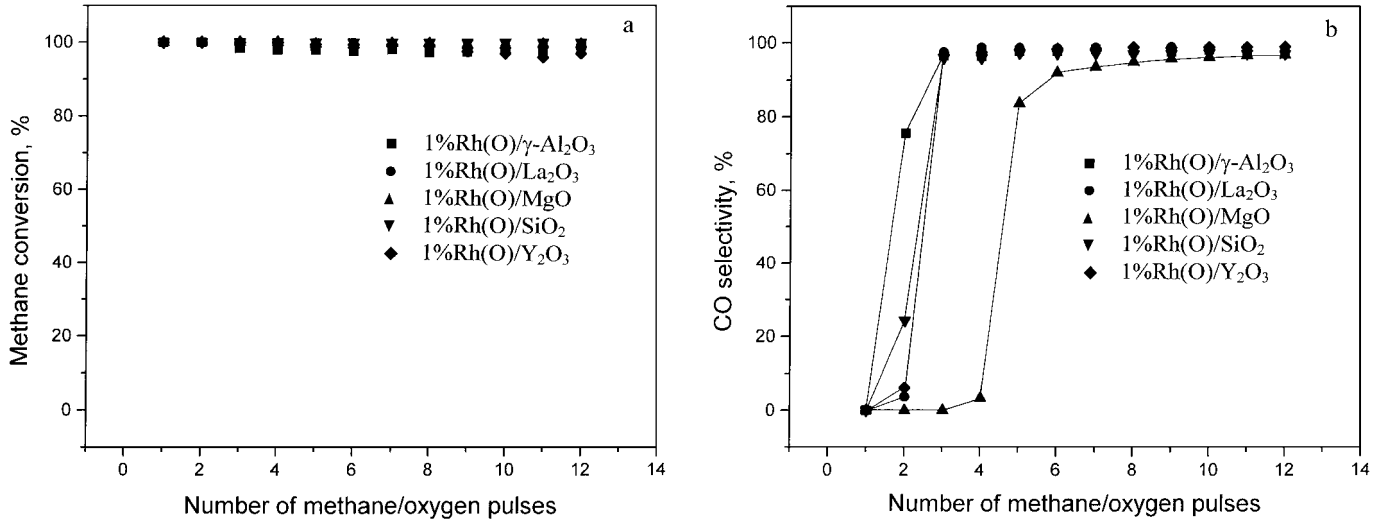

FIG. 2. Methane conversion (a) and CO selectivity (b) against the number of CH_4/O_2 (2/1) pulses over the irreducible-oxide-supported Rh catalysts at 750°C.

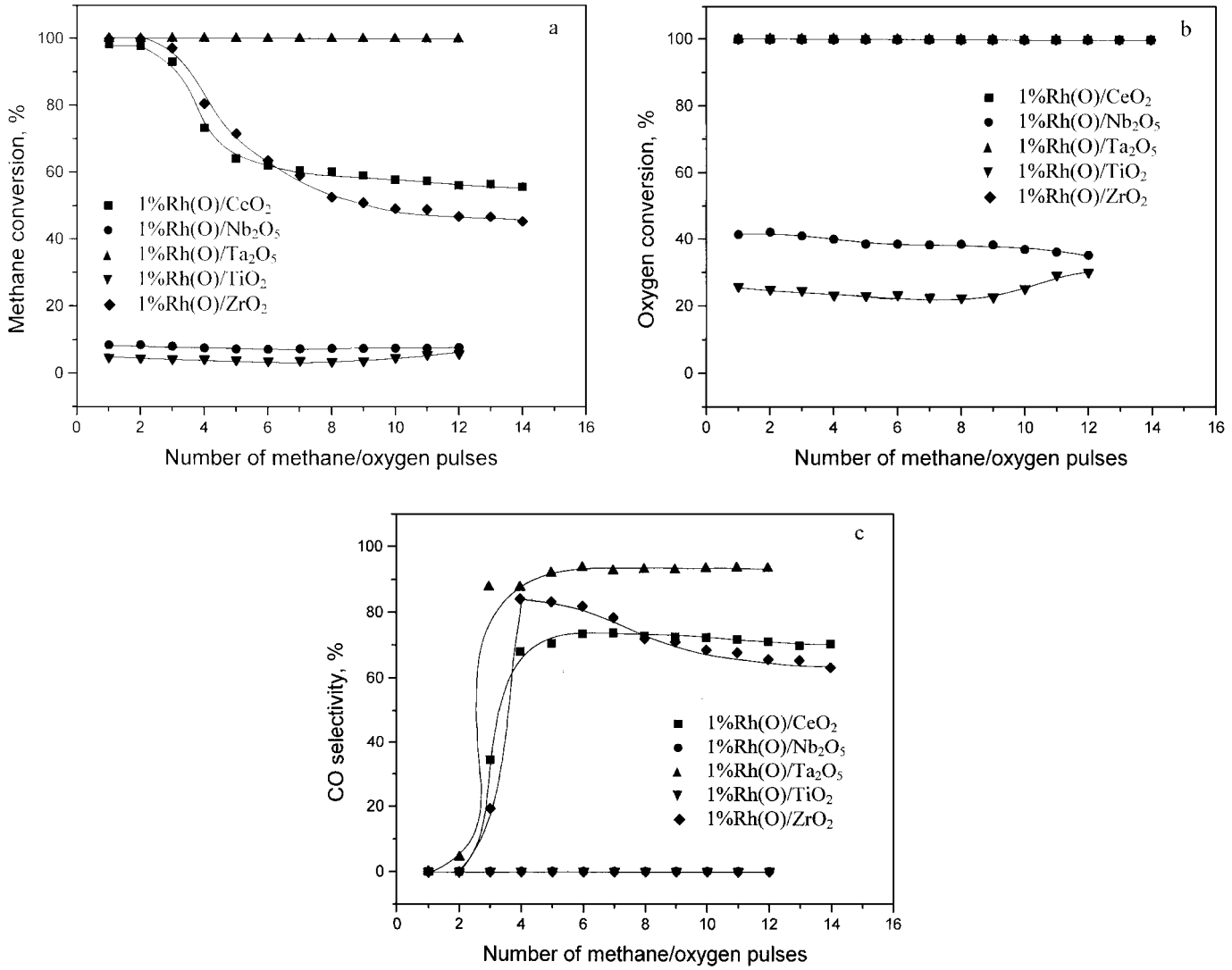

FIG. 3. Methane conversion (a), oxygen conversion (b), and CO selectivity (c) against the number of CH_4/O_2 (2/1) pulses over the reducible-oxide-supported Rh catalysts at 750°C. (Remark: ■, ▲, and ◆ are overlapping in b; and ● and ▼ in c.)

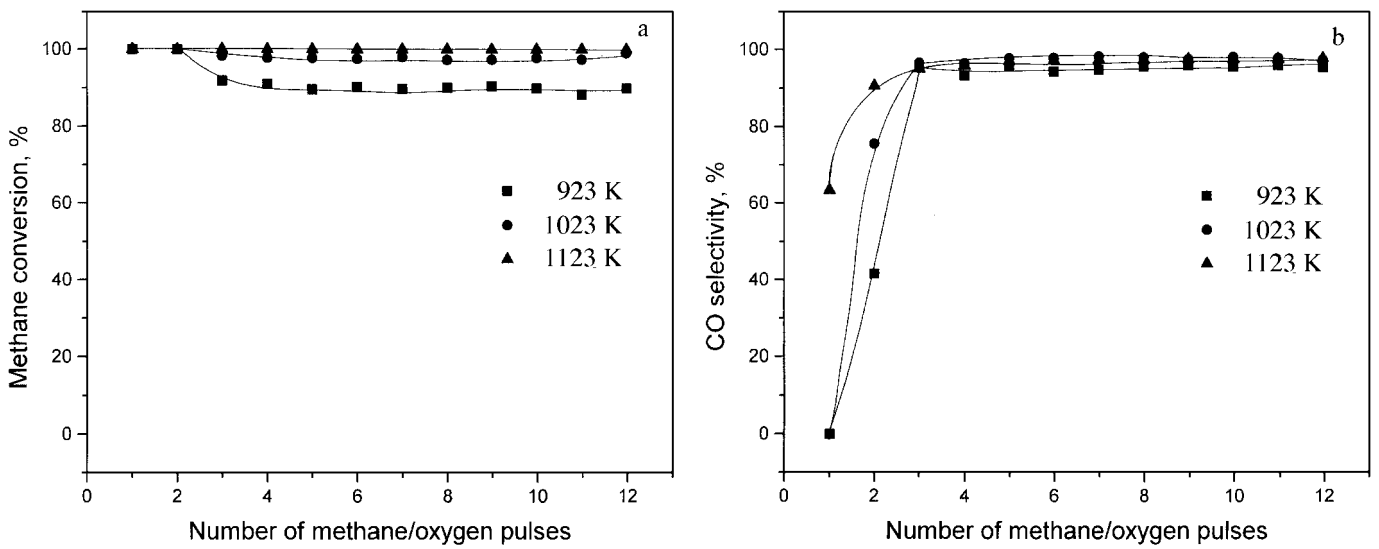

FIG. 4. Methane conversion (a) and CO selectivity (b) against the number of CH_4/O_2 (2/1) pulses over the 1% Rh(O)/γ-Al_2O_3 at 650, 750, and 850°C.

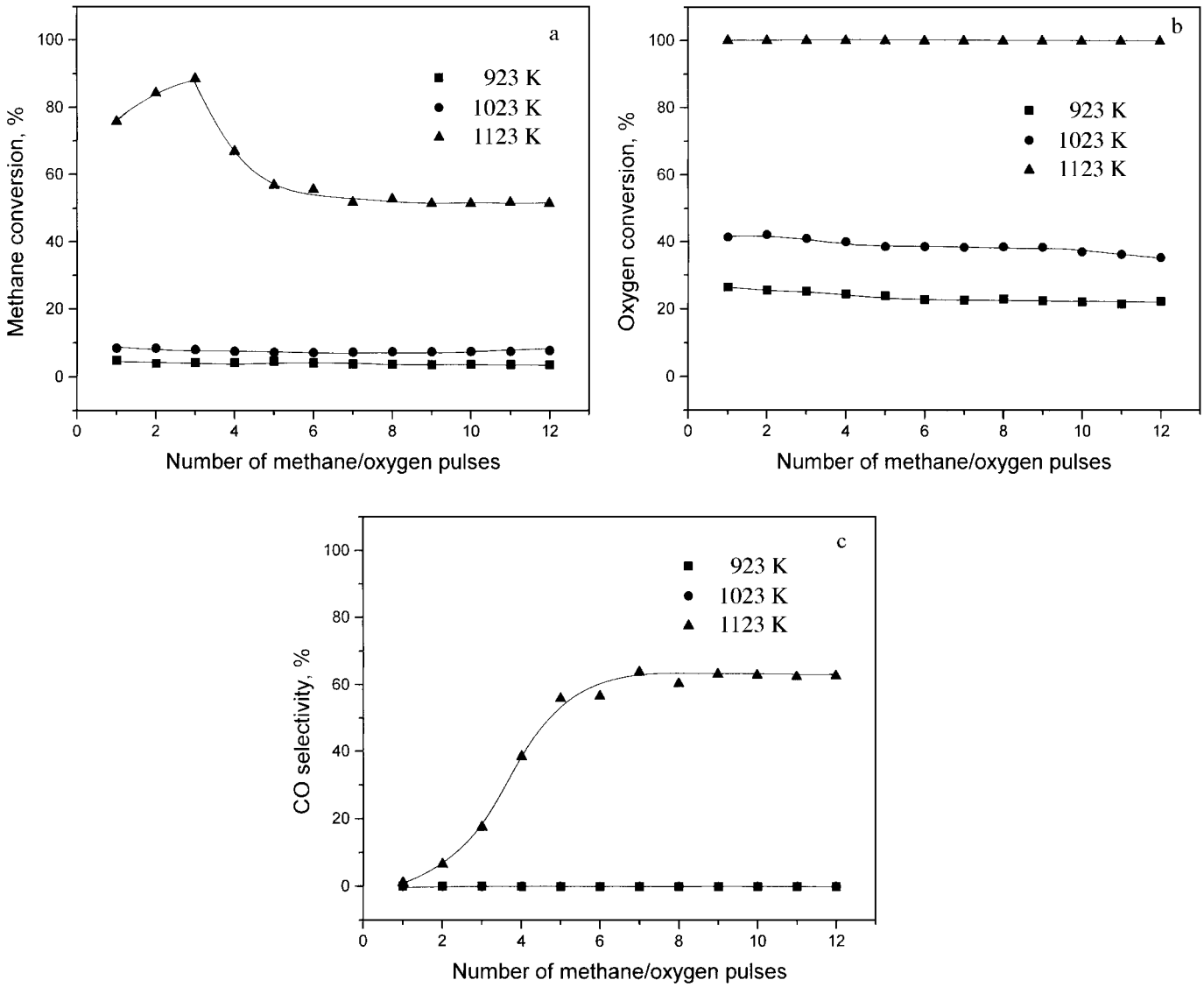

FIG. 5. Methane conversion (a), oxygen conversion (b), and CO selectivity (c) against the number of CH_4/O_2 (2/1) pulses over the 1% $Rh(O)/Nb_2O_5$ at 650, 750, and 850°C. (Remark: ■ and ● are overlapping in c.)

and the methane and oxygen conversions were very low. However, when the reaction temperature was increased to 850°C, the CO selectivity increased gradually with the increase in the number of pulses, indicating that the higher temperature activated the catalyst and induced the partial oxidation of methane. However, even at this high temperature, the CO selectivity remained much lower than that over the irreducible-oxide-supported rhodium catalysts. Similar results were observed over the TiO_2-supported catalyst. These results are again consistent with those of the continuous flow reaction (Table 1).

3.3. Physico-Chemical Characterization

After the calcined catalysts were reduced with H_2, the exposed metal surface areas were determined by CO chemisorption. As shown in Table 1, over the reducible-oxide-supported Rh catalysts, the exposed metal surface areas are much lower than those over the irreducible-oxide-supported ones.

TPR experiments were performed for all the calcined irreducible-oxide-supported catalysts and for the reducible Ta_2O_5 one. As shown in Fig. 6, the TPR peak temperature increased in the sequence

$$SiO_2 \leq \gamma\text{-}Al_2O_3 \leq Ta_2O_5 < Y_2O_3 \ll La_2O_3 < MgO.$$

XRD analysis was conducted for γ-Al_2O_3-, La_2O_3-, and MgO-supported rhodium catalysts, which provided high activities and selectivities with high stability (Fig. 1). Because the rhodium content of 1 wt% was too low for the XRD analysis, 10 wt% Rh(O)/support samples were prepared.

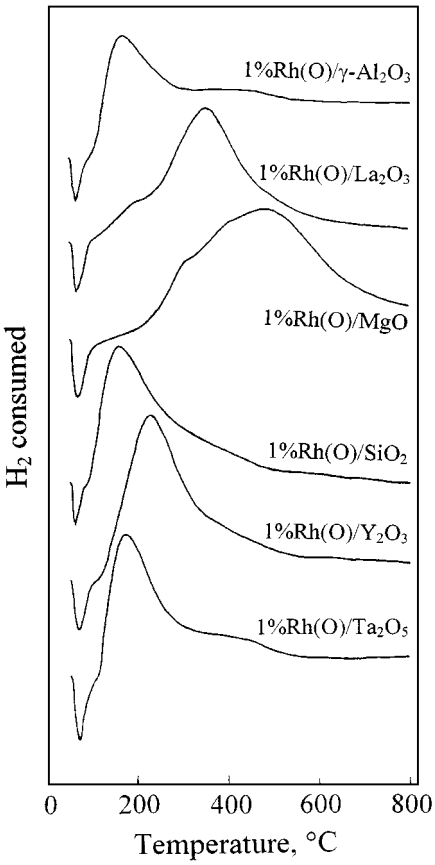

FIG. 6. TPR profiles of 1% Rh(O)/M_xO_y.

As shown in Table 3, Rh_2O_3, $LaRhO_3$ and Rh_2O_3 (minor), and $MgRh_2O_4$ were detected over the 10 wt% Rh(O)/γ-Al_2O_3, 10 wt% Rh(O)/La_2O_3, and 10 wt% Rh(O)/MgO, respectively. $LaRhO_3$ has the structure of a perovskite and $MgRh_2O_4$ the structure of a spinel.

4. DISCUSSION

4.1. Effect of Support

As shown in Table 1, the activity of rhodium strongly depends on the support. The irreducible supports provide, in general, much higher activities and selectivities to CO and H_2 than the reducible ones. As an exception, the reducible Ta_2O_5 provided activity and selectivities comparable to the irreducible support Y_2O_3. No simple, direct correlation between the catalytic activity (methane conversion) and the exposed metal surface area was found.

TABLE 3

Data and Assignments of XRD Patterns of Calcined 10% Rh(O)/M_xO_y Catalysts

Catalysts	d (Å)	Assignments
10% Rh(O)/Al_2O_3	1.39, 1.96; 2.50, 2.68, 1.70	γ-Al_2O_3; Rh_2O_3
10% Rh(O)/La_2O_3	2.93, 1.95, 3.34, 1.74, 1.64; 2.76, 3.45; 2.60, 2.79	La_2O_3; $LaRhO_3$; Rh_2O_3(minor)
10% Rh(O)/MgO	2.09, 1.48, 1.21, 1.27; 2.53, 4.76, 2.09, 1.48, 2.42	MgO; $MgRh_2O_4$

As shown in Table 1, after the calcined reducible-oxide-supported Rh catalysts were reduced with H_2, the exposed metal surface areas were much lower than those observed over the irreducible-oxide-supported ones. One possible explanation is that the rhodium metal particles were partially covered by islets of reduced oxide. Experimental evidence for the burying by the suboxide TiO_x, formed through the reduction of the TiO_2 support, of the metal particles was brought with regard to the so-called strong metal–support interactions (32, 33). The migration of TiO_x over the exposed surface of the metal particles takes place because it decreases the free energy of the system (32b). Indeed, depending upon the crystal face, Rh has a surface energy at room temperature between 2.5×10^3 and 2.9×10^3 erg/cm^2, while Ti has a value of 1.7×10^3 erg/cm^2 (35). TiO_2 is expected to have a smaller surface energy than Ti, because an oxide has a lower surface energy than the metal (32b). While TiO_x may have a somewhat higher surface energy than TiO_2, the reduction generates vacancies, which enhance the surface diffusion and hence the migration of TiO_x over the exposed surface area of the metal particles. The partial coverage of a rhodium particle by species generated via the reduction of support decreases the number of active metal sites, thus resulting in a lower activity. Even though no direct correlation between activity and the exposed metal surface area is evident (Table 1) for the reducible-oxide-supported catalysts, the Nb_2O_5 supported Rh catalyst, which has the lowest exposed metal surface area after reduction, exhibited the lowest catalytic activity.

As shown in Table 2, combustion of methane took place when a mixture of CH_4 and O_2 was pulsed over the pure (free of Rh) reducible or irreducible metal oxides. However, over the irreducible-oxide-supported catalysts, the combustion reaction played a minor role (Fig. 2), because CH_4 and O_2 can be easily activated by the metal sites and converted to CO and H_2, and the combustion which takes place over the oxide sites is much slower. With the exception of Ta_2O_5, which behaved like the irreducible oxides, for the reducible-oxide-supported catalysts, the selectivity to CO_2 was 100% over Nb_2O_5- and TiO_2-supported catalysts and important over the CeO_2- and ZrO_2-supported ones (Fig. 3). Under the continuous reaction conditions, a part of the suboxide generated via the reduction of a reducible oxide migrated over the metal surface, where it was reoxidized by the oxygen contained in the feed gas. The suboxide (or oxide) present on the surface of the metal particles decreases the number of active rhodium sites, thus resulting in a lower activation of CH_4 and O_2 and conversion to CO and H_2; on the other hand, the combustion reaction is promoted

by the numerous oxide sites available. As revealed by Table 2, the pure Ta_2O_5 exhibited negligible activity for the combustion reaction of CH_4 and O_2 at 750 and 850°C compared to other reducible oxides. One possible reason might be that the ignition temperature in the presence of this oxide is higher than the temperature employed. In addition, the surface energy of Ta is 2.7×10^3 erg/cm^2, hence comparable to that of Rh and much higher than that of Ti (35). Even though Ta_2O_5 is reducible (much less than the other reducible oxides (32a)), the surface energy of Ta_2O_x is not sufficiently smaller than that of Rh to allow the former to migrate as a strong surface active agent over the surface of the metal particles. For these reasons the Ta_2O_5-supported rhodium catalyst exhibited much higher catalytic activity and selectivities to H_2 and CO than the other reducible oxides.

The sintering is very harmful for the supported metal catalysts, because the aggregation of metal crystallites decreases the number of active sites and also accelerates the carbon deposition since large metal ensembles stimulate the carbon deposition. In general, the strong interactions between metal and support are beneficial in the stabilization of the tiny metal crystallites (32b). As shown in Fig. 1, among the irreducible supports, γ-Al_2O_3-, La_2O_3-, and MgO-supported Rh catalysts provided a stable catalytic activity for the partial oxidation of methane at the high GHSV of 720000 ml g^{-1} h^{-1}. As shown in Fig. 6, the TPR peak temperatures of La_2O_3- and MgO-supported Rh catalysts are much higher than those of SiO_2-, γ-Al_2O_3-, Ta_2O_5-, and Y_2O_3-supported ones, indicating that there are much stronger interactions between rhodium oxide and La_2O_3 or MgO. In the latter two catalysts, $LaRhO_3$ and $MgRh_2O_4$ were identified, respectively, in the precursor catalysts by means of XRD (Table 3). These compounds are most likely responsible for the stability of the La_2O_3- and MgO-supported Rh catalysts. Nevertheless, while no strong interactions between rhodium oxide and γ-Al_2O_3 could be identified (Fig. 6 and Table 3), the γ-Al_2O_3-supported Rh catalyst was stable. A possible explanation is as follows: Under the reaction conditions of methane partial oxidation, the atmosphere in the reactor is both reductive and oxidative. Sintering is stimulated by the reductive atmosphere and the oxidative atmosphere stimulates redispersion (32b). When on average they compensate one another, the system can remain stable and this probably happens with the Al_2O_3-supported catalysts but not with the SiO_2- and Y_2O_3-supported catalysts.

4.2. Active Sites for the Partial Oxidation of Methane

Many researchers concluded that the metal is the active site for the partial oxidation of methane (6, 12, 26, 36–46). New evidence is given below in this paper.

As shown in Fig. 5, over the precalcined Nb_2O_5- (similar results have been obtained with TiO_2) supported Rh catalysts, only total oxidation products, CO_2 and H_2O, were formed in the pulse reaction between CH_4 and O_2 at 650 and 750°C; both methane and oxygen conversions remained constant with increasing number of pulses. The following two steps are most likely involved in this reaction:

1. The reaction between methane and surface lattice oxygen, which gives CO_2 and H_2O and reduces Rh_2O_3 to Rh^0,

$$3CH_4(g) + 8Rh^{3+} + 12[O^{2-}] \rightarrow 3CO_2(g) + 6H_2O(g) + 8Rh^0 + 12[*]. \quad [4]$$

2. Reoxidation of Rh^0 by the gaseous oxygen, which restores the catalyst to its original state,

$$2Rh^0 + 3O_2 + [*] \rightarrow 2Rh^{3+} + 3[O^{2-}], \quad [5]$$

where [*] denotes an anion vacancy.

However, when the temperature was increased to 850°C, during the first pulse the oxygen was completely converted and the methane conversion was about 75% ($\gg$25%, 25% corresponding to the complete combustion based on the oxygen present in the feed) with a CO_2 selectivity close to 100%. This means that some of the oxygen was provided by the lattice. Consequently, one can conclude that at 850°C metallic rhodium was generated according to reaction [4]. The amount of metallic rhodium increased with the number of CH_4/O_2 pulses until a steady state was reached. Since the selectivity to CO increased in parallel with the number of metal sites, it is clear that the latter is responsible for the partial oxidation of methane. As shown in Fig. 4, over γ-Al_2O_3 and other irreducible-oxide-supported Rh catalysts, metallic rhodium can be generated even at 650°C during the first pulse of CH_4/O_2, thus inducing the methane partial oxidation at a lower temperature than over the reducible oxides. Since the rate of reaction is directly related to the state of the Rh particles, the relative ease of generation of metallic rhodium for irreducible-oxide-supported catalysts implies that they have much higher activity for syngas formation compared to the reducible-oxide-supported ones. This conclusion is in agreement with the continuous flow reaction experiments (Table 1).

5. CONCLUSION

The effect of support on the partial oxidation of methane over rhodium-based catalysts was investigated. The performance of the supported Rh catalyst is strongly affected by the support. The reducible oxides are, in general, not suitable supports for rhodium for this reaction. A possible reason is that the suboxide generated via the reduction of the reducible oxides migrates onto the surface of the metal particles, decreasing the number of active rhodium sites and hence the catalytic activity and promoting the combustion reaction. Among the irreducible oxides, MgO provides

the highest catalytic activity with high product selectivity and stability. The strong interactions between rhodium and magnesium oxides (especially the formation of $MgRh_2O_4$) are responsible for the high stability of MgO-supported Rh catalyst. Metallic rhodium can be generated via the reaction between methane and rhodium oxide (or rhodium-containing compound) even in the presence of oxygen and induces the partial oxidation of methane. Therefore, it is clear that the metal sites are responsible for the partial oxidation of methane.

REFERENCES

1. Rostrup-Nielsen, J. R., *Catal. Today* **18**, 305 (1993).
2. Fox, J. M., III, *Catal. Rev. Sci. Eng.* **35**, 169 (1993).
3. Hickman, D. A., and Schmidt, L. D., *J. Catal.* **138**, 267 (1992).
4. Bhattacharaya, A. K., Breach, J. A., and Chand, S., *et al., Appl. Catal. A Gen.* **80**, L1 (1992).
5. Hickman, D. A., Haupfear, E. A., and Schmidt, L. D., *Catal. Lett.* **17**, 223 (1993).
6. Hickman, D. A., and Schmidt, L. D., *Science* **259**, 343 (1993).
7. Torniainen, P. M., Chu, X., and Schmidt, L. D., *J. Catal.* **146**, 1 (1994).
8. Bharadwaj, S. S., and Schmidt, L. D., *Fuel Processing Technol.* **42**, 109 (1995).
9. Witt, P. M., and Schmidt, L. D., *J. Catal.* **163**, 465 (1996).
10. Nakagawa, K., Ikenaga, N., and Suzuki, T., *et al., Appl. Catal. A Gen.* **169**, 281 (1998).
11. Prettre, M., Eichner, C., and Perrin, M., *Trans. Faraday Soc.* **43**, 335 (1946).
12. Dissanayake, D., Rosynek, M. P., Kharas, K. C. C., and Lunsford, L. H., *J. Catal.* **132**, 117 (1991).
13. Vermeiren, W. J. M., Blomsma, E., and Jacobs, P. A., *Catal. Today* **13**, 427 (1992).
14. Choudhary, V. R., Mamman, A. S., and Sansare, S. D., *Angew. Chem. Int. Ed. Engl.* **31**, 1189 (1992).
15. Choudhary, V. R., Rajput, A. M., and Prabhakar, B., *J. Catal.* **139**, 326 (1993).
16. Choudhary, V. R., Uphade, B. S., and Mamman, A. S., *Catal. Lett.* **32**, 387 (1995).
17. Chu, Y., Li, S., and Lin, J., *et al., Appl. Catal. A Gen.* **134**, 67 (1996).
18. Choudhary, V. R., Uphade, B. S., and Mamman, A. S., *J. Catal.* **172**, 281 (1997).
19. Miao, Q., Xiong, G., and Sheng, S., *et al., Appl. Catal. A Gen.* **154**, 17 (1997).
20. Lu, Y., Liu, Y., and Shen, S., *J. Catal.* **177**, 386 (1998).
21. Tang, S., Lin, J., and Tan, K. L., *Catal. Lett.* **51**, 169 (1998).
22. Drago, R. S., Jurczyl, K., Kob, N., Bhattacharyya, A., and Masin, J., *J. Catal.* **51**, 177 (1998).
23. Chen, P., Zhang, H. B., Lin, G. D., and Tsai, K. R., *Appl. Catal. A Gen.* **166**, 343 (1998).
24. Ashcroft, A. T., Cheetham, A. K., and Foord, J. S., *et al., Nature* **344**, 319 (1990).
25. Jones, R. H., Ashcroft, A. T., and Waller, D., *et al., Catal. Lett.* **8**, 169 (1991).
26. Slagtern, A., and Olsbye, U., *Appl. Catal. A Gen.* **110**, 99 (1994).
27. Choudhary, V. R., Uphade, B. S., and Belhekar, A. A., *J. Catal.* **163**, 312 (1996).
28. Lago, R., Bini, G., Pena, M. A., and Fierro, J. L. G., *J. Catal.* **167**, 198 (1997).
29. Nakamura, J., Aikawa, K., Sato, K., and Uchijima, T., *Catal. Lett.* **25**, 265 (1994).
30. Nakagawa, J., Anzai, K., and Matsui, N., *et al., Catal. Lett.* **51**, 163 (1998).
31. Bodke, A. S., Bharadwaj, S. S., and Schmidt, L. D., *J. Catal.* **179**, 138 (1998).
32. (a) Stevenson, S. A., Raupp, G. B., Dumesic, J. A., Tauster, S. J., and Baker, R. T. K., *in* "Metal–Support Interactions in Catalysis, Sintering, and Redispersion" (S. A. Stevenson, J. A. Dumesic, R. T. K. Baker, and E. Ruckenstein, Eds.), p. 34. Van Nostrand–Reinhold, New York, 1987; (b) Ruckenstein, E., in "Metal–Support Interactions in Catalysis, Sintering, and Redispersion" (S. A. Stevenson, J. A. Dumesic, R. T. K. Baker, and E. Ruckenstein, Eds.), p. 297. Van Nostrand–Reinhold, New York, 1987.
33. Minachev, Kh. M., and Shpiro, E. S., *in* "Catalyst Surface: Physical Methods of Studying" (Kh. M. Minachev and E. S. Shapiro, Eds., translated from the Russian by G. Leib), p. 255. CRC Press, Boca Raton, FL, 1990.
34. Dissanayake, D., Rosynek, M. P., and Lunsford, J. H., *J. Phys. Chem.* **97**, 3644 (1993).
35. Personal information from Dr. W. F. Egelhoff, Jr., Magnetic Material Group, NIST, Gaithersburg, MD 20899.
36. Buyevskaya, O. V., Wolf, D., and Baerns, M., *Catal. Lett.* **29**, 249 (1994).
37. Hu, Y. H., and Ruckenstein, E., *Catal. Lett.* **34**, 41 (1995).
38. Hu, Y. H., and Ruckenstein, E., *J. Catal.* **158**, 260 (1996).
39. Au, C. T., Wang, H. Y., and Wan, H. L., *J. Catal.* **158**, 343 (1996).
40. Wang, D. Z., Dewaele, O., Groote, A. M. D., and Froment, G. F., *J. Catal.* **159**, 418 (1996).
41. Au, C. T., and Wang, H. Y., *Catal. Lett.* **41**, 159 (1996).
42. Mallens, E. P., Hoebink, J. H. B. J., and Marin, G. B., *J. Catal.* **167**, 43 (1997).
43. Au, C. T., and Wang, H. Y., *J. Catal.* **167**, 337 (1997).
44. Looij, F. van, and Geus, J. W., *J. Catal.* **168**, 154 (1997).
45. Hu, Y. H., and Ruckenstein, E., *J. Phys. Chem. A* **102**, 230 (1998).
46. Hu, Y. H., and Ruckenstein, E., *J. Phys. Chem. A* **102**, 10568 (1998).